Tropical Atlantic Sea Surface Temperature Forcing of Quasi-Decadal Climate Variability over the North Atlantic–European Region

L. TERRAY AND C. CASSOU

Climate Modelling and Global Change Project, CERFACS/SUC URA1875, Toulouse, France

(Manuscript received 10 December 2001, in final form 1 May 2002)

ABSTRACT

Effects of Atlantic sea surface temperature (SST) anomalies on the North Atlantic low-frequency atmospheric variability are examined by analyzing two ensembles of integrations of the ARPEGE general circulation model (GCM) forced with differently configured observed SSTs and sea ice extents (SIE) over the 1948–98 period. An attempt is made to separate the forced atmospheric response from internal atmospheric variability by using a signal-to-noise maximizing empirical orthogonal function (EOF) analysis. This method yields an estimate of the most detectable common forced response given the knowledge of internal variability provided by the ensemble. Applying the algorithm to North Atlantic atmospheric model data leads to an atmospheric response associated with a tripole pattern in North Atlantic SSTs. The spatial structure of the forced response, which is most consistent in winter, shows a dipole pattern in mean sea level pressure projecting onto the North Atlantic Oscillation. Examination of other atmospheric variables shows a very coherent signal with a quasi-barotropic signature. Additional atmospheric integrations with idealized SST anomaly patterns demonstrate the primary role of the tropical North Atlantic SST anomalies in generating the forced response. The physical mechanism involves related changes in tropical convection, Hadley circulation, and the modulation of the stationary and transient planetary-scale waves by the low-frequency variability in subtropical winds induced by the persistent tropical circulation anomalies.

1. Introduction

During the past few decades there has been considerable effort devoted to obtaining a better understanding of natural climate variability in the North Atlantic region on monthly to interdecadal timescales. However, the mechanisms governing these climatic fluctuations are still not fully understood. A number of recent studies have sought to identify the nature of the variability at different timescales by analyzing both observational records and results of climate model simulations. Yet, one does not know whether coupled dynamical processes play a role or if climate variability arises through internal instabilities in one climate system component that imprints its changes on the other components. There has been a great deal of work trying to confirm which of these two hypotheses is valid for a given timescale.

On monthly timescales, there is strong evidence that much of the observed ocean variability is driven by atmospheric forcing. First, the dominant spatial scales of the observed SST anomalies are much larger than the ocean's Rossby radius of deformation and comparable to the observed scale of low-frequency atmospheric anomalies. Second, lag-correlation analyses clearly indicate that the atmosphere is leading the ocean in the extratropics (Wallace and Jiang 1987). Thermodynamic and wind-induced mechanisms such as buoyancy and momentum air–sea exchange, entrainment, and vertical mixing have been proposed to explain how the extratropical atmosphere forces upper-ocean temperature anomalies on monthly to seasonal timescales (Frankignoul 1985; Cayan 1992a,b). Once the latter have been generated, the surface turbulent heat flux acts as a negative feedback with an averaged magnitude of 20 W m^{-2} K^{-1} (Frankignoul et al. 1998). On interannual timescales, the persistence of SST anomalies may be due to the reemergence mechanism (Alexander and Deser 1995). Upper-ocean temperature anomalies created over a deep mixed layer in winter may be preserved in the summer thermocline and reappear at the surface in the following fall or winter.

On interdecadal timescales, the ocean dynamics could be responsible for sustaining or modulating the atmospheric variability modes. The dominant mode of atmospheric behavior in the North Atlantic sector is called the North Atlantic Oscillation (NAO) and is characterized by a large-scale alternation of atmospheric mass with centers of action near the Icelandic low and the Azores high. It is robustly present in every month of the year (although it is more pronounced during winter;

Corresponding author address: Dr. L. Terray, Climate Modelling and Global Change Project, CERFACS, 42, Avenue Gaspard Coriolis, 31057 Toulouse Cedex, France.
E-mail: terray@cerfacs.fr

Barnston and Livezey 1987) and accounts for the largest fraction of interannual variability in monthly North Atlantic sea level pressure (SLP; Rogers 1990). Several authors have defined climatic indexes using SLP anomalies near the Azores and Iceland for the last 150 years or so, and searched for potential oscillatory behavior in NAO time series (Rogers 1984; Hurrell 1995; Jones et al. 1997). Even longer records for the NAO index have been constructed from tree-ring-based data (1701–1980; Cook et al. 1998) and Greenland ice cores (Appenzeller et al. 1998). Spectral analyses show that the NAO has a rich spectrum of variability, including quasi-biennal, decadal, and interdecadal spectral peaks (Hurrell and van Loon 1997). However, the statistical significance of these peaks is not clearly established. For instance, it has been argued that the NAO SLP time series spectrum is indistinguishable from a weakly red noise process (Wunsch 1999) or that it has long-memory process properties (Stephenson et al. 1999). Furthermore, wavelet analysis of the proxy data–based indexes shows essentially a white spectrum but for the last century where concentration of the spectral power at a 70-yr period occurs leading to slight reddening (Appenzeller et al. 1998).

However, the reddening of the observed spectra, albeit rather slight, could suggest a potential link with a slow component of the climate system. Atmospheric GCMs forced by climatological SSTs display fluctuations that resemble the spatial structure of observed modes of variability such as the NAO, which strongly suggests that these modes are intrinsic modes of the atmosphere (Marshall and Molteni 1993). On the other hand, the reddening of the observed spectrum is not captured in these experiments that display a white spectrum for the NAO-like variability mode (Terray and Cassou 2000). Furthermore, there are strong *physical* arguments suggesting that the Atlantic Ocean may play an active role in modulating climate on interdecadal timescales. Bjerknes (1964) investigated SST and SLP variability in the North Atlantic and showed that interdecadal warming corresponded to an enhancement of the prevailing westerly winds over the positive SST anomalies. This is in clear contrast with the seasonal to interannual warming case where positive SST anomalies coincide with a weakening of the westerlies. Kushnir (1994) demonstrated that, while the picture of local air–sea interaction does apply to seasonal to interannual SST anomalies, interdecadal ones may result from a basin-scale dynamical interaction between the large-scale oceanic circulation and the overlying atmosphere.

The situation is not as clear for interannual to decadal fluctuations. Ensembles of atmospheric GCM integrations forced by the history of SST variations show ensemble-mean skill in reproducing the NAO variability on interannual timescales (Rodwell et al. 1999; Mehta et al. 2000). As the SST forcing is global, it cannot be concluded from these experiments in which oceanic regions are responsible for the atmospheric forced response. At near-decadal timescales, there is strong evidence of slow (only few cm s^{-1}) propagation of SST anomalies along the North Atlantic Current (NAC) at the boundary of the subtropical and subpolar gyres (Hansen and Bezdek 1996; Sutton and Allen 1997). However, there is not yet evidence for a strong atmospheric response to these midlatitude SST anomalies. Whether North Atlantic SST anomalies have an impact on the atmospheric circulation is a crucial point if one wants to explain low-frequency variations by invoking midlatitude ocean–atmosphere coupling. Many modeling studies have addressed this question by using idealized or observed SST anomaly patterns to force an atmospheric GCM (Palmer and Sun 1985; Kushnir and Lau 1992; Ferranti et al. 1994; Lau and Nath 1994; Peng et al. 1995; Kushnir and Held 1996). The picture emerging from these studies is a rather confusing one as summarized in Peng et al. (1997). Low-resolution models tend to exhibit either no response, a shallow baroclinic response with a low-level trough and an upper-level ridge downstream of a positive SST anomaly, or an equivalent barotropic response with a trough growing with height. On the contrary, high-resolution model experiments with positive SST anomaly give a downstream anomalous ridge with an equivalent barotropic structure. Peng and Whitaker (1999) have shown the important role of the transient eddies vorticity fluxes in forcing the barotropic response. This vertical structure of the response is similar to the one that is observed to covary with anomalous SSTs. However, even in the high-resolution model experiments, large differences remain regarding the amplitude of the response, its seasonality, and the role of nonlinearities. The only agreement lies in the fact that the atmospheric response to extratropical anomalies is weak but not negligible. The typical signal-to-noise ratio for the interannual response to midlatitude anomalous SST is between 0.1 and 0.2 in the current generation of models, while it increases for longer timescales (Kushnir et al. 2002).

Another cause for low-frequency atmospheric variability over the North Atlantic can have its origin in the tropical Atlantic Ocean variability (TAV) through tropical–extratropical connection. The TAV is known to have several modes coming from different sources. First, the tropical North Atlantic SST variability is linked to (El Niño–Southern Oscillation) ENSO-related fluctuations through the tropospheric bridge and effects of altered northeasterly winds on evaporative and sensible heat fluxes (Enfield and Mayer 1997; Klein et al. 1999; Saravanan and Chang 2000). Another mode of TAV is the so-called dipole SST mode: its meridional structure is revealed by the correlation between tropical Atlantic SST and rainfall over northern Nordeste (NNE) Brazil (Nobre and Shukla 1996). As suggested by some model studies, this SST dipole could arise from a local air–sea feedback mechanism between the wind-induced latent heat flux and SST (Chang et al. 1997). Furthermore, it seems to weakly operate at the decadal timescale while interannual fluctuations are mainly nondipolar in character (Enfield et al. 1999).

Few modeling studies have documented possible mechanisms for the tropical–extratropical linkage in the Atlantic. A recent study by Robertson et al. (2000) suggests that the NAO may be remotely influenced by tropical South Atlantic SST variability. Specifically, anomalous SSTs in the tropical South Atlantic can induce meridional shifts in the Hadley cell formed by convection over the Amazon and subsidence over the subtropical North Atlantic, which can then affect the NAO mode. Another study based on an AGCM coupled to a slab ocean has shown that tropical Atlantic SST fluctuations selectively enhance variance of the NAO (Watanabe and Kimoto 1999). The latter study also pointed out the central role played by the midlatitude transient eddy feedback in generating the extratropical height anomalies associated with the dominant modes of tropical Atlantic SST variability. There is also modeling evidence for a relationship between cross-equatorial SST gradient variability and the extratropics through a barotropic teleconnection (Okumura et al. 2001). The latter study also suggested potential positive feedback mechanisms relying on wind-induced evaporation and low-level stratiform clouds in the subtropics. Finally, while the subtropical part of the SST tripole plays a subtantial role in many modeling experiments, the extratropical Atlantic SST anomalies also influence the atmospheric response and the effects are not additive (Sutton et al. 2001).

This work addresses the following focal questions: Do the Atlantic SSTs influence the atmospheric low-frequency variability over the extratropical North Atlantic–European (NAE) region? Which are the key oceanic regions having the dominant forcing effect onto the atmosphere? What are the amplitude and the signal-to-noise ratio of the atmospheric response? What are the mechanisms responsible for a significant atmospheric response, if any? To investigate in detail the NAE atmospheric response to observed interannual SST fluctuations, the following strategy was followed. First, two ensembles of atmospheric GCM integrations were performed. The first one is an ensemble of eight atmospheric simulations forced by the global observed SST and sea ice extents (SIE) for the period 1948–98. A signal-to-noise maximizing EOF analysis was then applied in order to identify the dominant forced response and the associated forcing pattern as well as its time evolution. A second ensemble of four atmospheric simulations was also performed with the observed SST field in the Atlantic only and the climatology elsewhere. The same EOF analysis was also applied in order to confirm the initial results and to clearly separate the impact of the Atlantic SSTs. The forcing SST pattern emerging from these two ensembles of integrations was then used to force the atmospheric model in several anomaly experiments. The latter were used to understand the mechanisms behind the forced response and to investigate the comparative role of different regions of Atlantic SSTs.

The structure of the paper is as follows. Section 2 describes the atmospheric model, the experimental design, and the data preprocessing. Section 3 explains how to extract the dominant forced response from an ensemble of integrations and compares it to observations. Possible physical mechanisms underlying this SST forcing are discussed in section 4. Section 5 gives a summary and directions for future work.

2. The experimental design and data processing

a. The model and the used simulations

The atmospheric GCM used in the present study is derived from the ARPEGE/IFS forecast model and is described by Déqué et al. (1994). The present version uses a spectral T63 triangular horizontal truncation. Diabatic fluxes and nonlinear terms are calculated on a Gaussian grid of about 2.8° latitude by 2.8° longitude. The vertical is discretized over 31 levels (20 levels in the troposphere) using a progressive vertical hybrid coordinate extending from the ground up to about 34 km (7.35 hPa). Further details about the model physics package can be found in Cassou and Terray (2001b).

The multidecadal simulations used in this work are the same 8-member ensemble as the one described in Cassou and Terray (2001b). Each member was integrated from 1 January 1947 to 31 March 1998 with lower boundary forcing provided by a blend of two reconstructed Global Sea Ice and Sea Surface Temperature datasets (GISST; Rayner et al. 1997); namely, the GISST 2.3 from 1947 to 1982 and the new released GISST 3.0 package from 1983 to 1998. These simulations are of the Global Ocean–Global Atmosphere–type (GOGA) meaning that monthly observed SSTs are prescribed globally. The eight GOGA simulations differ only by their initial atmospheric conditions. In addition to the GOGA simulations, a 4-member ensemble of the Atlantic Ocean–Global Atmosphere–type (AOGA) is also analyzed in this work. The AOGA set of experiments are forced with the same SSTs except that the forcing is specified only in the Atlantic north of 45°S. There is a 10°-wide buffer zone in the Southern Atlantic where SSTs are gradually damped to the climatological values. Climatological SST monthly means are assigned elsewhere in the global oceans. All these simulations give a set of 50 complete years, the first simulated year being discarded in the subsequent analyses to account for the adjustment time of the land surface and atmospheric variables. The GOGA climatology and the model variables of interest are thoroughly described in Cassou and Terray (2001b) and compare reasonably well with that inferred from the National Centers for Environmental Prediction–National Center for Atmospheric Research (NCEP–NCAR) reanalysis. The latter paper also provides a preliminary description of the simulated forced variability as estimated from the GOGA ensemble mean (GOGA-EM). The GOGA-EM NAO index has a slightly red spectrum with energy concentration in a broad 3–8-yr band and is associated with SST fluctuations over both the tropical Pacific and the North Atlantic (Cassou and Terray 2001b).

b. *Treatment of data*

Monthly anomalies of atmospheric variables are obtained by substracting the 400 (8×50) yr climatology from the monthly data. Then, the standard seasonal means [December–January–February (DJF); MAM; JJA; SON] are constructed by averaging over a 3-month period. As this work is focused on low-frequency atmospheric fluctuations (with periods between 3 and 10 yr), these timescales are emphasized by removing any linear trend and low-pass filtering for each set of seasonal means. The filtering retains fluctuations with periods greater than 3 yr and uses a fourth-order Butterworth filter. Note however that the spatial structure of the dominant forced atmospheric variability modes presented in this paper is not sensitive to the low-frequency data filtering. The latter impacts the time evolution of the forced response by stressing quasi-decadal fluctuations. This work will concentrate on the winter (DJF) and spring (MAM) seasons that show the largest externally forced variance as depicted by the analysis of variance (ANOVA) analysis (Cassou and Terray 2001b). The subsequent analysis will be performed mostly on a North Atlantic (NATL) domain, from 10° to 80°N in latitude and from 90°W to 0° in longitude. The principal variable we analyze is the mean sea level pressure (MSLP).

3. Dominant forced response to sea surface temperature forcing

A common assumption in climate studies is to divide the atmospheric variability into an internal part, generated by the nonlinear dynamics of the atmosphere, and an external part forced by the time-varying surface boundary conditions (SST and SIE). While, in nature, this separation is not necessarily physically meaningful, it appears to be a sensible starting point as one is interested in timescales longer than those of the chaotic components of the climate system. In this context, the internal part of the variability is referred to as the ''noise'' as it is uncorrelated to the external forcing. The external part is often termed the ''signal'' or the ''forced response'' and can be defined as the component of the variability that depends solely on the external forcing, independent of the initial conditions. Identifying the external part of the variability is important as it can provide potentially predictable signals. This determination of the forced response at midlatitudes is difficult because the signal is often much weaker than the noise. Furthermore, the internal variability can have strong variance in the phase-space direction of the forced response that contaminates the estimation of the signal. Ensemble averaging can be used to separate the signal from the noise and gives a biased estimate of the true forced response (if the ensemble size is infinite, the ensemble mean gives the true forced response). In practice, the ensemble size is often too small to get an unbiased estimate of the forced response through direct ensemble averaging and the internal variability strongly contributes to the variability of the ensemble mean. Given a finite number of ensemble simulations, the issue is how to maximize the signal-to-noise ratio (SNR) in order to get the most predictable signal, which is not necessarily the largest.

a. *Signal-to-noise maximizing EOF analysis*

The concept of optimal pattern detection can be used to detect the dominant forced response in an ensemble of atmospheric GCM simulations. Venzke et al. (1999) applied the signal-to-noise maximizing EOF algorithm developed by Allen and Smith (1997) to extract the dominant MSLP forced response in the North Atlantic sector from an ensemble of six simulations of the first Hadley Centre Atmospheric General Circulation Model (HadAM1). The same analysis was also applied to study the effects of tropical Atlantic SST anomalies on the atmospheric circulation simulated by an ensemble of integrations with the Climate Community Model (CCM3; Chang et al. 2000). The reader is referred to Venzke et al. (1999) for a detailed description of the optimal detection algorithm. A brief outline is given hereafter. The main steps of the algorithm are the following: first, any spatial correlation in the noise contaminating the ensemble mean is removed by applying a prewhitening filter (PWF) which makes the noise spatially white. In order to build the PWF, one needs an estimate of the leading EOFs of the noise covariance matrix. As in Venzke et al. (1999), it is estimated from the deviations of each ensemble member from the ensemble mean. Furthermore, in order to avoid poorly sampled noise EOFs, it is necessary to confine the analysis to the K leading EOFs. The truncation level, K, is determined using the technique mentioned in Venzke et al. (1999). The results shown in this paper are robust if K is chosen between 20 and 30. After applying the PWF, an EOF analysis of the ensemble mean is performed to extract the dominant forced response. The algorithm gives a spatial pattern that is an unbiased estimate of the first EOF of the external part of the variability (i.e., the dominant forced response). The associated time series [or principal component (PC)] is called the optimized PC (OPC) and gives the time evolution of the dominant forced response. The algorithm yields also optimal filter patterns (OPF) that optimally discriminate between the signal and the noise (in other words, they have large amplitude when the SNR is high). In contrast with standard EOF-based methods, the signal-to-noise

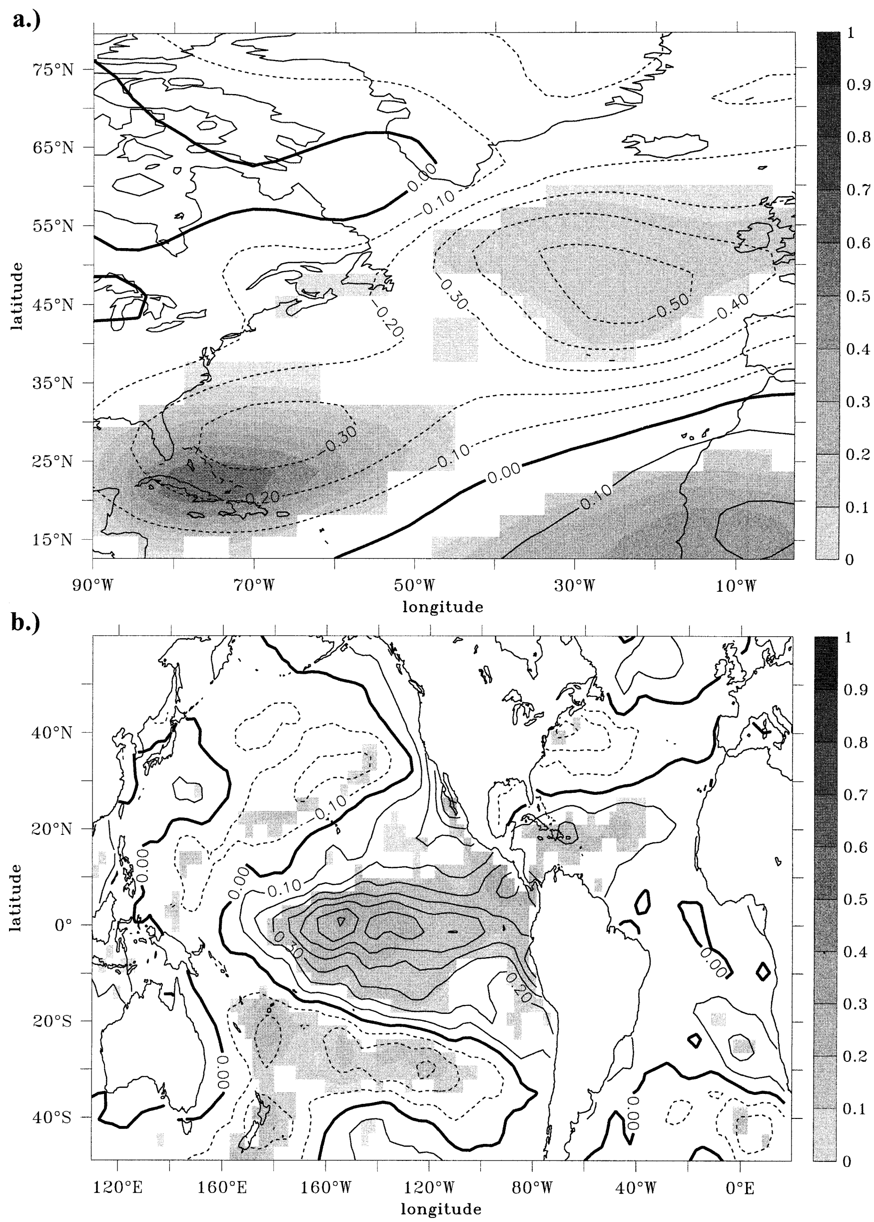

FIG. 1. (a) Regression coefficients (hPa; contour lines) and fraction of total ensemble-mean variance explained (shaded where significant at the 95% confidence level) by the regression of GOGA ensemble-mean winter mean SLP data onto the associated OPC. (b) Regression coefficients (K; contour lines) and fraction of total variance explained (shaded where significant at the 95% confidence level) by the regression of observed SST anomalies onto the associated OPC.

maximizing EOF analysis does not use the SST field to identify the forced response. The surface forcing pattern is obtained a posteriori by regressing the surface forcing field (SST) onto the OPC.

b. The dominant forced responses over the North Atlantic sector

1) THE ENSO INFLUENCE

The algorithm was applied to the winter and spring seasonal means of the MSLP from the GOGA simulations. The dominant signal is the remote response to ENSO activity. For instance, Fig. 1 shows the leading mode of SST forced MSLP variability in DJF with the associated SST forcing field for the NATL domain. The SST map clearly shows an ENSO signal in the tropical eastern and central Pacific associated with a tilted band of low pressure anomalies over the North Atlantic. The MSLP pattern is very similar to the one obtained in Venzke et al. (1999) with different relative magnitudes for the two main centers of action. In our experiment, the main center of action is located over the central

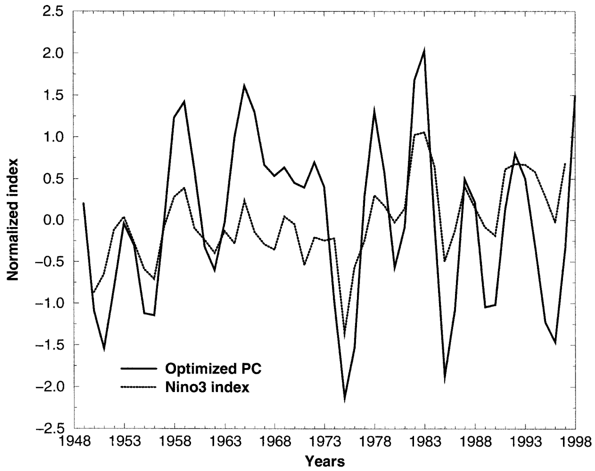

FIG. 2. OPC obtained by projection of GOGA ensemble-mean winter mean SLP data onto the optimal filter and low-pass-filtered (3 yr) Niño-3 index. Both time series have been normalized.

North Atlantic and not in the subtropics. This may well be due, as noted in Cassou and Terray (2001b), to an overestimated eastward extension of the Pacific North American (PNA) pattern in the ARPEGE model during the winter season. A similar analysis for the spring season gives a MSLP pattern in close agreement with the one in Venzke et al. (1999). Figure 2 presents the time evolution of the dominant forced response for the winter season together with a low-pass filter (3 yr) of the Niño-3 index. The OPC is clearly dominated by interannual fluctuations characteristic of ENSO variability (the two time series are correlated at 0.83, which is significant at the 99% level allowing for persistence).

2) THE ATLANTIC SST FORCING

As one is interested by possible local forcing through the Atlantic SSTs, the atmospheric part of the variability that is linearly induced by ENSO was removed from the analyzed dataset. Precisely, the regression of the GOGA MSLP data with the Niño-3 index was computed. The signal-to-noise maximizing EOF analysis was then repeated with the ''ENSO removed'' data (the residuals of the regression analysis). Figure 3 shows the leading atmospheric MSLP forced response and the related SST forcing pattern for both the winter and spring seasons. The dominant winter MSLP response over the NATL domain has a stronger than usual subtropical high pressure center and a deeper than normal Icelandic low, characteristic of a positive NAO phase. Again, the MSLP spatial pattern is close to the one found by Venzke et al. (1999) and exhibits a similar asymmetry in amplitude between the two centers of action. It is slightly shifted southward and more central in our case, thereby bearing a stronger resemblance to the canonical NAO pattern. The significance of the response and the amount of explained forced variance is high in the Tropics, weaker at midlatitudes, and not significant around the Icelandic low region. The associated SST forcing pattern exhibits the familiar tripole structure that has been described for instance in Deser and Blackmon (1993) and Sutton and Allen (1997). The regression pattern is significant at the 95% level over a large part of the tropical North Atlantic, while it is not detectable over the two northern branches of the tripole. This slightly differs from Venzke et al.'s results where the midlatitude branch was quite significant and the tropical one had weaker amplitude. Two additional centers also appear over the central tropical and central North Pacific. No clearly significant MSLP anomalies are found to be associated with these Pacific SSTs (not shown). The winter GOGA OPC is significantly correlated with the observed NAO index as defined by the principal component time series of the leading EOF of the winter MSLP anomalies over the NAE region. If the NAO index is low-pass filtered (retaining periods greater than 3 yr), the correlation is 0.61 and is significant at 99% level with 16 degrees of freedom. With no filtering, the correlation is still 0.46 and is significant at the 95% level allowing for persistence. Although the atmospheric fluctuations are mostly dominated by the NAO intrinsic variability, these results suggest that a weak but not negligible (around 20%) fraction of the interannual NAO variance can be considered as a response to SST forcing.

For the spring season, the MSLP forced response is not as coherent spatially. It exhibits a band of negative anomalies from Greenland to the British Isles associated with a zonal dipole in the subtropics (with negative anomalies off the Florida coast and positive ones along the West African coast). The SST forcing pattern displays the tripole (with weak amplitude) and is only detectable off the West African coast. These results disagree with those of Venzke et al. where the spring response was found to be the most consistent.

3) THE AOGA EXPERIMENTS

Removing the effects of ENSO using linear regression onto the Niño-3 index is certainly a rough approximation. To confirm the results of the previous section, the signal-to-noise maximizing EOF analysis was also applied to the AOGA experiments where the observed interannual SST forcing is prescribed only in the Atlantic. Note that indirect ENSO effects can still be present in this set of simulations through the atmospheric bridge between the eastern Pacific and the western tropical North Atlantic (Klein et al. 1999). Figure 4 shows the leading mode of Atlantic SST forced MSLP variability for the DJF and MAM seasons as well as the associated SST forcing patterns. In winter, the MSLP spatial structure has a pattern close to that of the GOGA leading mode although the high-latitude center is shifted northwestward over Baffin Bay. The amplitude of the response is stronger at the midlatitude than its GOGA counterpart, while the regions of statistical significance have remarkable similarities. The associated SST pat-

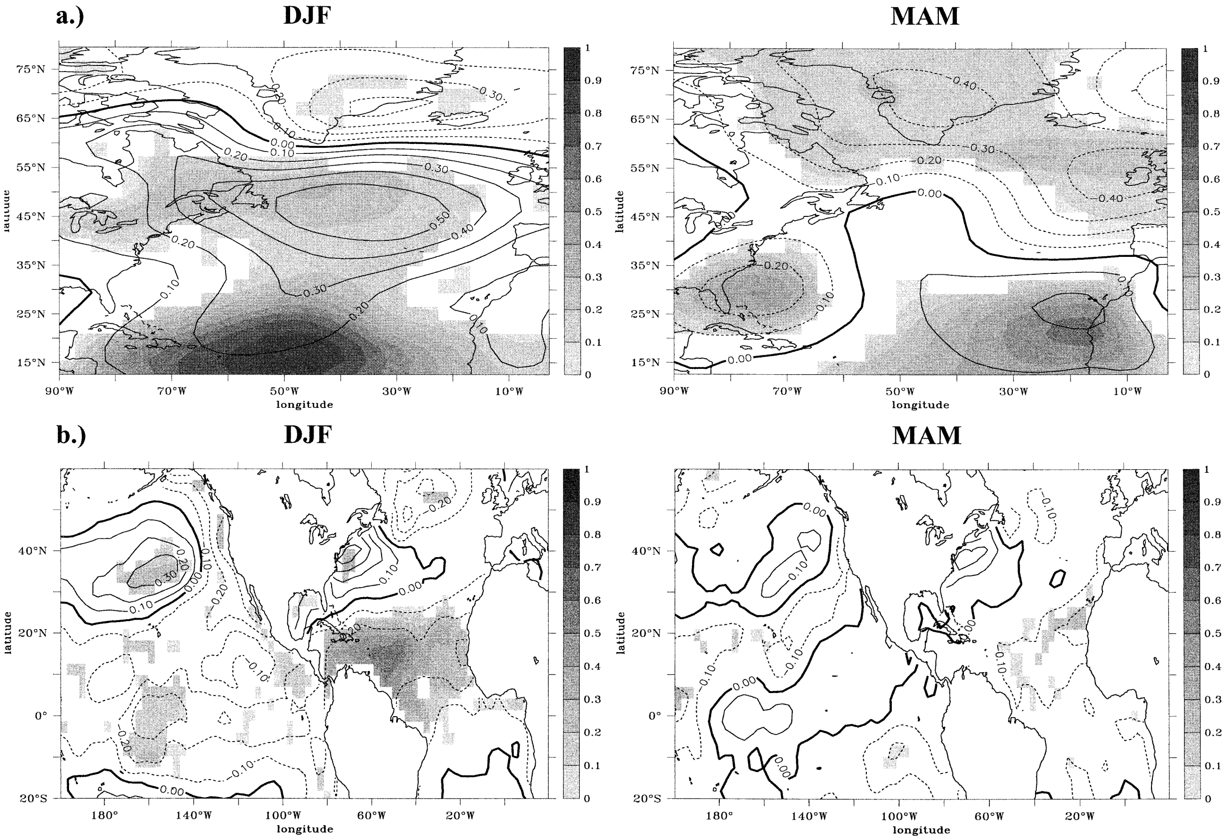

FIG. 3. (a) Regression coefficients (hPa; contour lines) and fraction of total ensemble-mean variance explained (shaded where significant at the 95% confidence level) by the regression of GOGA ''ENSO removed'' ensemble-mean winter and spring mean SLP data onto the associated OPC. (b) Regression coefficients (K; contour lines) and fraction of total variance explained (shaded where significant at the 95% confidence level) by the regression of observed SST anomalies onto the associated OPC.

tern bears a striking resemblance to that resulting from the GOGA analysis and suggests again the central role played by the tropical North Atlantic SSTs in generating the atmospheric response. In spring, the MSLP response differs from the GOGA one with anomalies of the same sign in the Tropics and off Newfoundland associated with anomalies over northern Europe of the opposite sign. Inspection of the SST forcing pattern suggests again the influence of the Atlantic tripole with its tropical lobe being the only statistically significant region. The amount of explained forced MSLP variance (for both DJF and MAM) is high in the Tropics, weaker at midlatitudes, and small at high latitudes. Examination of the temporal evolution of the forced responses shows that the AOGA winter OPC is strongly correlated to that deduced from the GOGA ENSO removed data (the correlation between the two time series is 0.78, which is significant at the 99% level with 10 degrees of freedom; Fig. 5). The AOGA winter OPC is also correlated to its spring counterpart (correlation of 0.81, which is significant at the 99% level with 10 degrees of freedom). The AOGA winter OPC exhibits quasi-decadal fluctuations (with periods between 6 and 8 yr) superimposed on a low-frequency trend. Negative phases of the NAO seem to be favored in the first 20 yr while the positive phase is dominant from 1970 onward. The major role of the southern part of the tripole in generating the forced response is confirmed by the high correlation between the AOGA winter OPC and the tropical North Atlantic (TNA) index as defined in Enfield et al. (1999; Fig. 6). This suggests that the dominant forced atmospheric response over the NAE region in the AOGA simulations originates mainly from SST fluctuations in the tropical North Atlantic.

To further demonstrate the tropical Atlantic SST role in forcing an NAO-type response over the NAE region, we have applied the climate regime methodology to the AOGA dataset (Martineu et al. 1999). A clustering scheme has been used to partition the total cloud of simulated atmospheric states into a given number of classes or clusters. Each individual atmospheric state is the realization of one particular event (one month of a given winter and a given AOGA simulation) for a given atmospheric variable. Concatenated AOGA experiments yield 480 atmospheric states (40 years $\times$ 3 months $\times$ 4 simulations) on which EOF filtering is applied in order to reduce the dimensionality of the system after projection onto the few leading modes (here the first 10

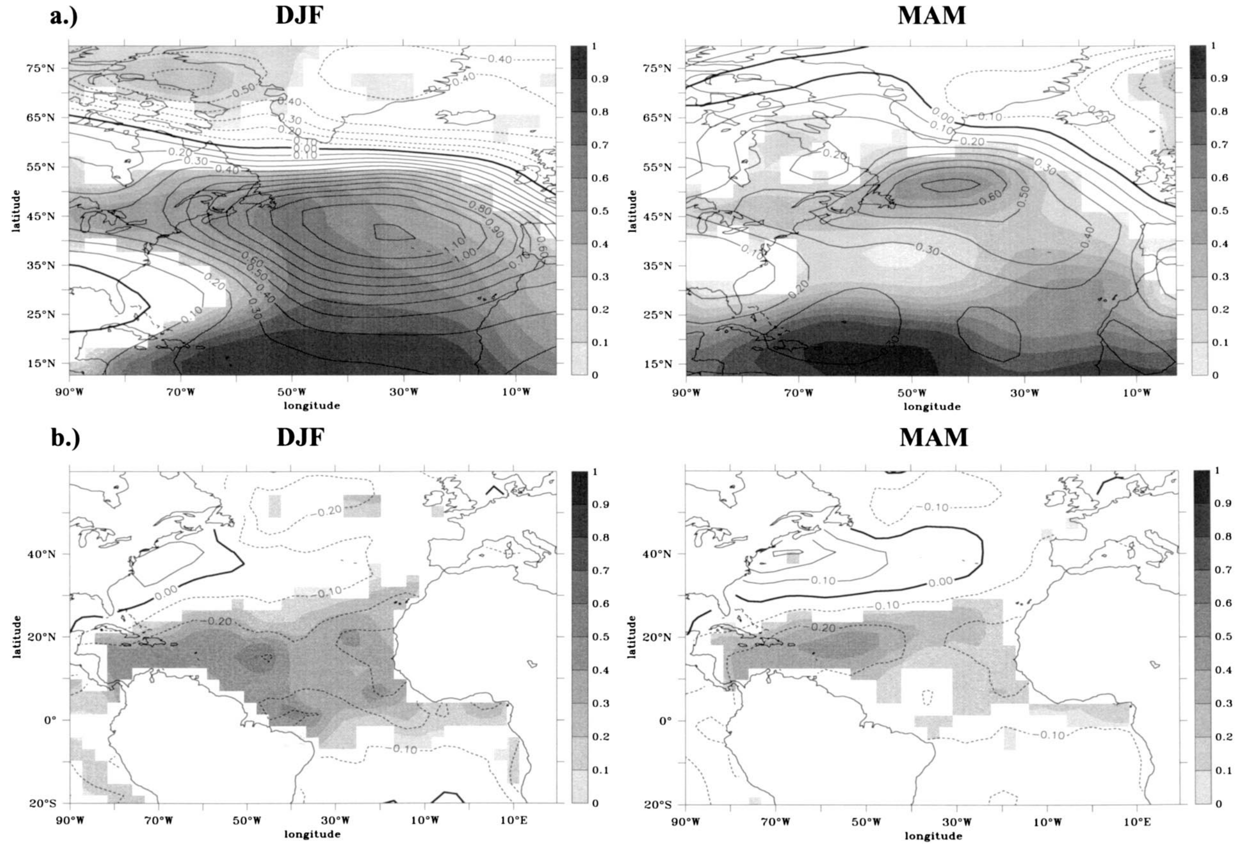

FIG. 4. As in Figs. 3a,b, but for the AOGA ensemble mean and associated OPC.

EOFs have been retained as they explained more then 90% of the variance). The algorithm is based on the k-means clustering method as detailed in Michelangeli et al. (1995) and is applied to the 480 MSLP field maps over the NATL domain. Given a prescribed number of clusters k, the goal of the algorithm is to find a partition of the dataset into k clusters that minimizes the sum of variance within the clusters. The Euclidian distance is used as the similarity measure. The optimal number of

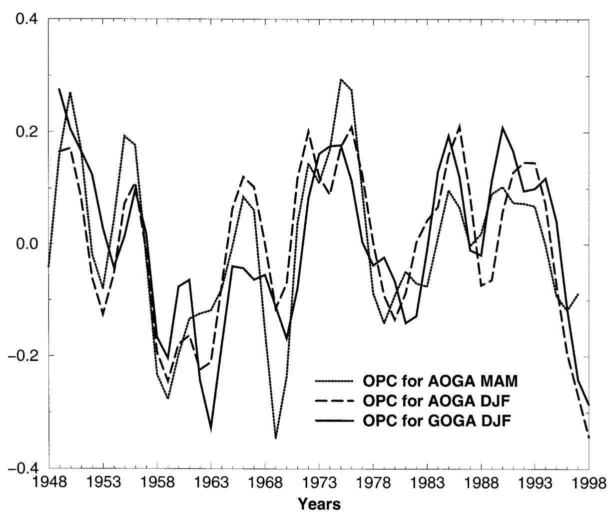

FIG. 5. OPC for the AOGA ensemble (winter and spring seasons) and for the ENSO-removed GOGA ensemble (winter only).

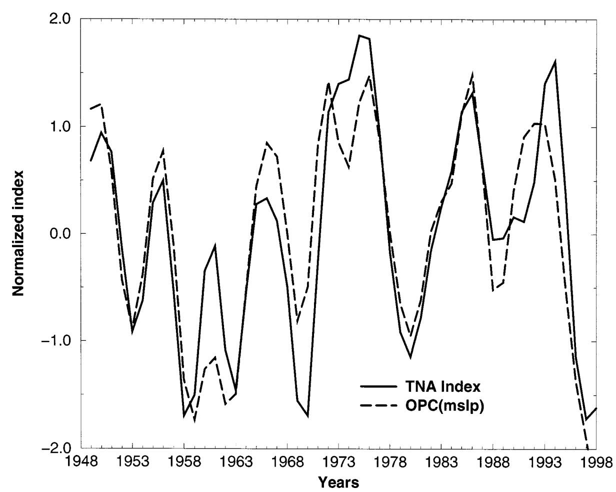

FIG. 6. OPC obtained by projection of AOGA ensemble-mean winter mean SLP data onto the associated optimal filter and low-pass-filtered (3 yr) tropical North Atlantic index. Both time series have been normalized.

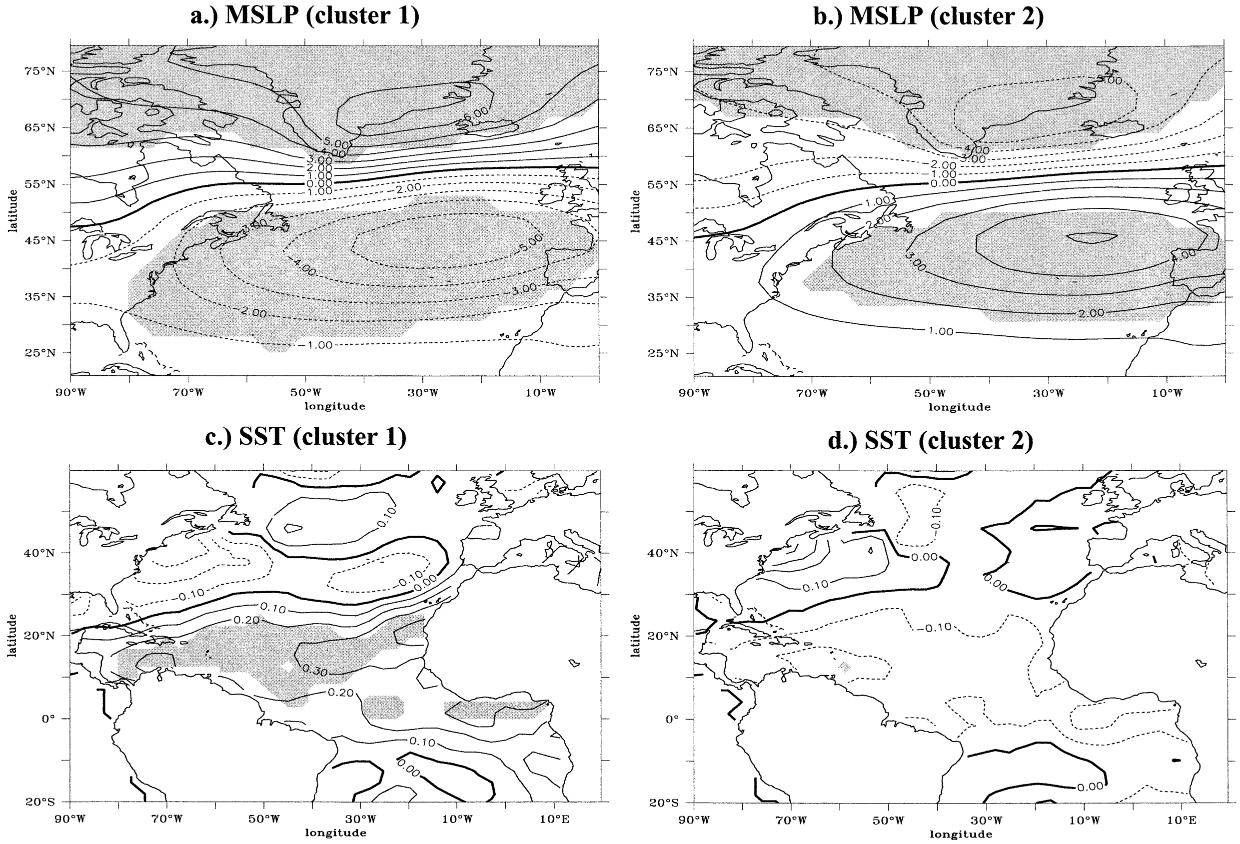

FIG. 7. Composite maps associated with the two climate regimes resulting from the application of the *k*-means clustering algorithm to the mean SLP (hPa) unfiltered AOGA winter monthly means (DJF) for (a), (b) mean SLP (hPa) and (c), (d) SST (K). Shading indicates statistical significance using a two-tailed *t* test at the 95% confidence level.

clusters k is found by using a reference noise model (first-order Markov process) that provides confidence thresholds for a classifiability index. The time occurrence of the resulting clusters can then be used to build composites for any atmospheric or forcing (SST) variables. The selection of events for the composite analysis is based on outputs from the hypergeometrical statistical test that defines the years significantly represented in each cluster (Martineu et al. 1999). The clustering analysis yields $k = 2$ and the resulting composites for MSLP and SST are shown in Fig. 7. The composite for the first cluster is characterized by a north–south dipole with a positive anomaly over Greenland and corresponds to the negative phase of the NAO (Fig. 7a). Conversely, the second cluster composite resembles the positive phase of the NAO (Fig. 7b). The associated SST composites depict the North Atlantic tripole with statistical significance restricted to the tropical part of the SST pattern related to the negative NAO phase (Figs. 7c,d). Considering the fact that the AOGA simulations are forced simulations, these results do confirm the association between tropical Atlantic SST anomalies and the phases of the NAO. Furthermore, they suggest that this relationship is asymmetric. While the negative phase of the NAO is significantly associated with positive tropical Atlantic SST anomalies, the reverse relationship is much less clear. Possible reasons for this asymmetry are given in the next section.

c. *Sensitivity to the physical variable used in the optimization*

We have also applied the signal-to-noise maximizing algorithm to other atmospheric variables from the AOGA simulations such as the geopotential height at 500 hPa (Z500) as well as the zonal wind at 200 hPa (U200). The resulting time series for the winter season agree remarkably well with the MSLP OPC (Fig. 8a) and the associated SST patterns are also very similar (not shown). The spatial structure of the Z500 and U200 responses suggests the leading forced mode has a quasi-barotropic signature (Figs. 8b,c). The Z500 pattern exhibits a north–south-orientated dipolar structure that projects very strongly upon the simulated NAO pattern in its positive phase as depicted by the first EOF of the Z500 anomaly field (not shown). Similarly, the U200 response shows a strengthening of the subtropical jet over the Atlantic as well as a strengthening and northward shift of the main jet off the east coast of North America. The strengthening and splitting of the Atlantic

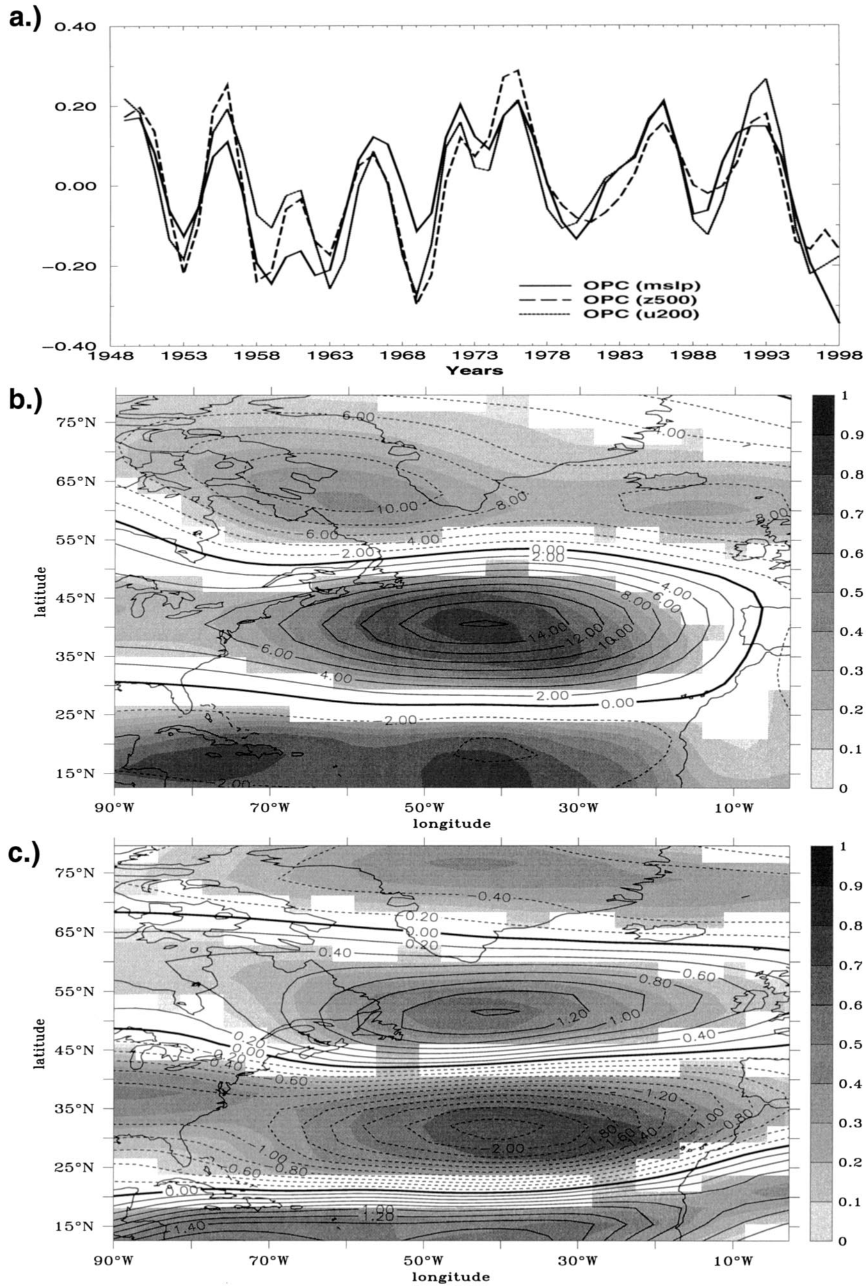

FIG. 8. (a) OPC for the AOGA ensemble winter mean SLP, 500-hPa geopotential height, and 200-hPa zonal wind. (b) Regression coefficients (*m*; contour lines) and fraction of total ensemble-mean variance explained (shaded where significant at the 95% confidence level) by the regression of AOGA ensemble-mean winter 500-hPa geopotential height data onto the associated OPC. (c) Same as in (b) but for 200-hPa zonal wind data. The regression coefficients are in m s^{-1} (contour lines).

jet is characteristic of the positive phase of the observed and simulated NAO (Cassou and Terray 2001a). These results indicate that the signal-to-noise maximizing EOF analysis has identified a vertically and physically coherent signal. Furthermore, the spatial signature of the forced response strongly projects onto the spatial structure of the main mode of internal variability as deduced from a 100-yr simulation with climatological SSTs. This suggests the following interpretation: the low-frequency influence of Atlantic SSTs onto the atmosphere over the NAE region could be interpreted in terms of changes in the frequency of occurrence of intrinsic atmospheric circulation regimes. This approach has been used in the climate change context to show that most of the recent

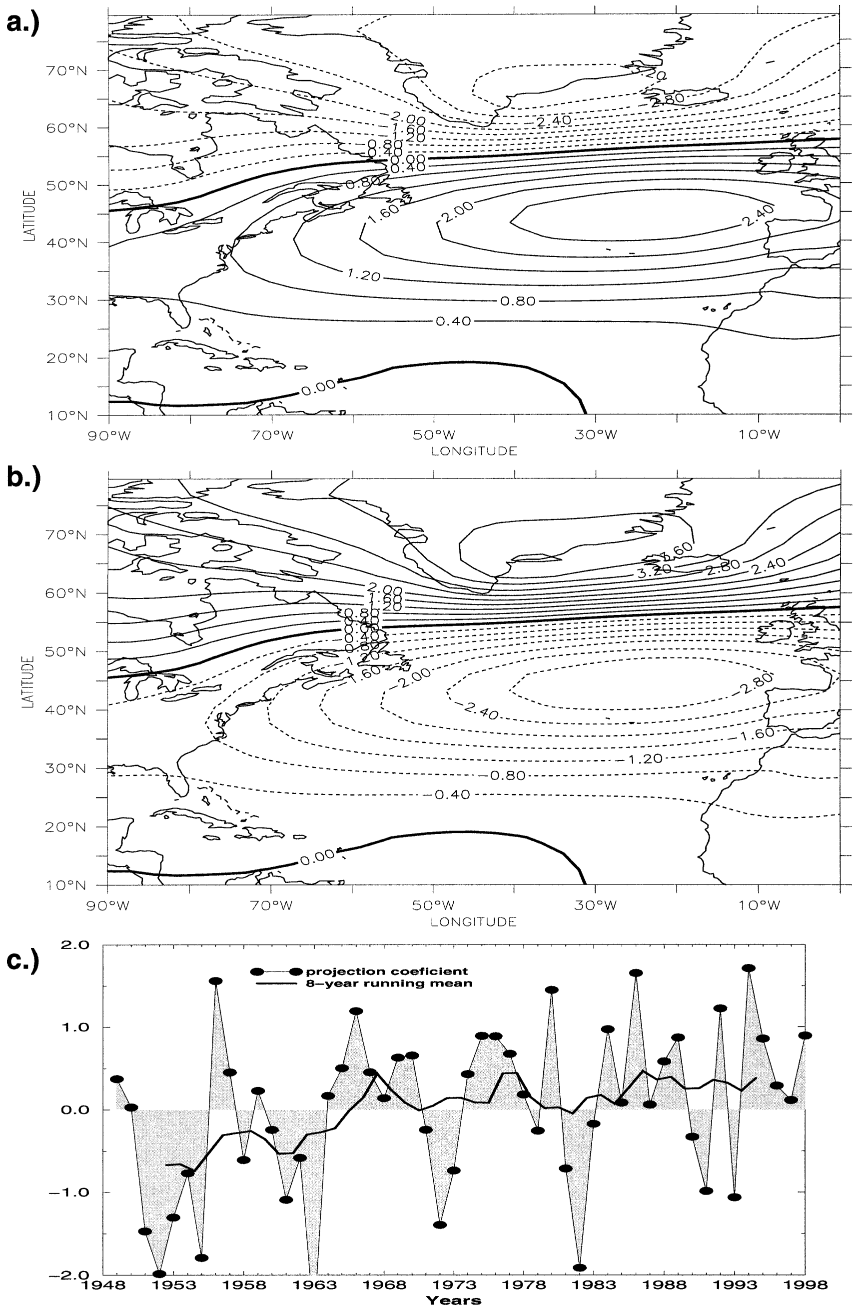

FIG. 9. (a), (b) Cluster centroids resulting from the application of the *k*-means clustering algorithm to the mean SLP (hPa) AOGA winter monthly means (DJF). The classified data have been detrended by retaining deviations from low-pass-filtered (periods greater than 3 yr) monthly means. (c) Projection coefficients of AOGA ensemble-mean nondetrended mean SLP data onto the cluster shown in (a). Filled circles represent seasonal average, and the black line is the 8-yr running mean.

observed warming can be understood in terms of an increase in the frequency of occurrence of a cluster representing the so-called cold ocean warm land (COWL) pattern (Corti et al. 1999). In order to test if the nonlinear picture outlined above applies to the Atlantic SST forcing, we have performed a cluster analysis of winter NAE 500-hPa geopotential height monthly means from the AOGA dataset for the 1949–98 period. The seasonal cycle has been removed and the data further detrended by applying a fourth-order Butterworth high-pass filter that retains fluctuations of periods less than 3 yr. Figure 9 shows the two clusters representing the two phases of

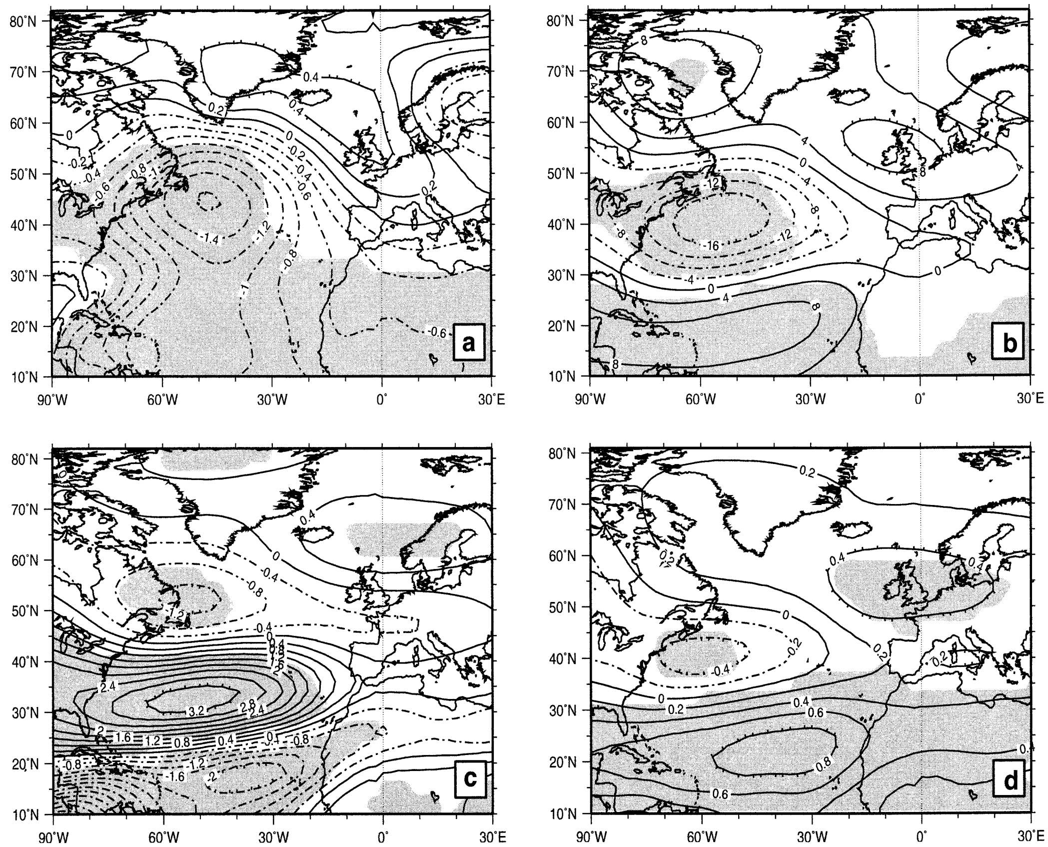

FIG. 10. Winter (DJF) difference field between the TAP (positive tropical SST anomalies) and TAN (negative tropical SST anomalies) for (a) mean SLP (hPa), (b) 500-hPa geopotential height (m), (c) 200-hPa zonal wind (m s^{-1}), and (d) 500-hPa temperature (K). Shading indicates statistical significance using a two-tailed *t* test at the 95% confidence level.

the simulated NAO as well as the time series of the projection coefficients of the nondetrended MSLP anomalies onto the cluster NAO$^+$ representing the positive NAO phase. The time series shows a clear upward low-frequency trend that is consistent with the increase in the frequency of occurrence of the NAO$^+$ regime. These results suggest that the recent low-frequency shift between the subperiods 1950–70 (regime NAO$^-$ dominant) and 1971–98 (regime NAO$^+$ dominant) can be understood in terms of a greater occurrence of a natural regime of NAE atmospheric intraseasonal–interannual variability. Furthermore, oceanic forcing arising from Atlantic SST fluctuations could be partially responsible for this shift.

4. Discussion of potential physical mechanisms

a. Role of tropical sea surface temperature anomalies

The results of the preceding sections suggest the leading role of tropical North Atlantic SST anomalies in generating a detectable atmospheric response over the NAE region in the ARPEGE model. To confirm this finding and to further understand the physical mechanisms responsible for this influence, a tropical SST anomaly pattern, identical to the one of Fig. 4b (which is associated with the most detectable atmospheric response), has been used to force 30-yr idealized simulations with the model. The seasonal cycle of the SST anomalies is as follows: from June to November, the climatology is prescribed. In winter (DJF) and spring (MAM), the SST patterns of Fig. 4b are added with a 1-month linear transition between every SST change. The SST anomalous pattern is restricted to the tropical North Atlantic (0°–30°N) and two simulations have been performed with the positive (TAP) and negative (TAN) versions of the SST anomaly. Maximum values of the SST forcing are about 1°C. Figure 10 shows the difference in DJF MSLP, Z500, U200, and temperature at 500 hPa (T500) between the TAP and TAN (TAD = TAP − TAN) experiments. In the following, it is assumed that the TAD fields represent the linear response to tropical North Atlantic anomalies (all the figures and related text describe the positive SST anomaly case). The spatial patterns are remarkably similar to those derived from the signal-to-noise maximizing EOF analysis, demonstrating the primary role of tropical North

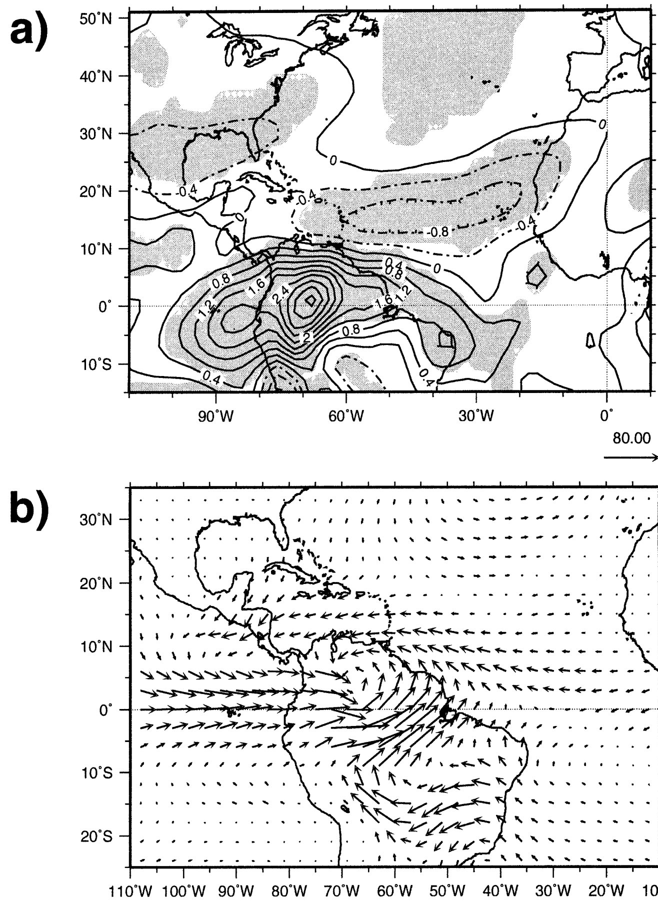

FIG. 11. Winter (DJF) difference field between the TAP and TAN for (a) 200-hPa wind divergence (10^{-6} s^{-1}) and (b) moisture transport (arrows) at 850-hPa (g kg^{-1} m s^{-1}). Shading indicates statistical significance using a two-tailed *t* test at the 95% confidence level.

Atlantic SSTs. However, it is worth noting that the simulated extratropical anomalies display a wave pattern (along a southwest–northeast great circle) reminiscent of a Rossby wave (Hoskins and Karoly 1981) and that projects onto the simulated NAO. The main difference is a secondary maximum located between Iceland and the British Isles (Fig. 10b). The vertical structure of the anomaly is baroclinic in the Tropics and essentially barotropic at mid- and high latitudes. The temperature pattern shows dynamical heating in the Tropics, cooling in midlatitudes, and warming at high latitudes throughout the troposphere, indicating increased poleward heat transport and reduced meridional temperature gradient. Note that the anomalous surface fluxes would tend to force the mid- and high-latitude branches of the classic SST tripole (not shown). The 200-hPa divergence field difference between the TAP and TAN experiments shows anomalous divergence and upward motion over the Amazonian region due to increased convection over the continent (Fig. 11a). Areas of anomalous 200-hPa convergence and subsidence, required by mass balance considerations, are located over the Gulf of Mexico and the southern United States as well as over a zonal belt across the tropical North Atlantic. Note that the latter is centered right above the prescribed SST anomaly pattern. The enhanced remote continental equatorial convection seems to be caused by an increased low-level moisture transport toward Amazonia (Fig. 11b). The anomalous supply of moisture has three different sources: the eastern Pacific, the South Atlantic and Brazil, and the tropical North Atlantic. The first two are dominated by anomalous advection of mean moisture while the last one is driven by moisture anomalies advected by the mean flow. These moisture anomalies are caused by enhanced evaporation over the tropical North Atlantic related to the warm SST anomalies. The upper-level anomalous divergent circulation anomalies tend to be localized rather than uniformly spread, which suggests a possible description in terms of anomalous regional Hadley-type cells. To support this hypothesis, zonally averaged cross sections of TAD zonal and meridional wind are presented for the western Atlantic. The TAD meridional circulation depicts anomalous convergence in the upper troposphere around 30°N and divergence

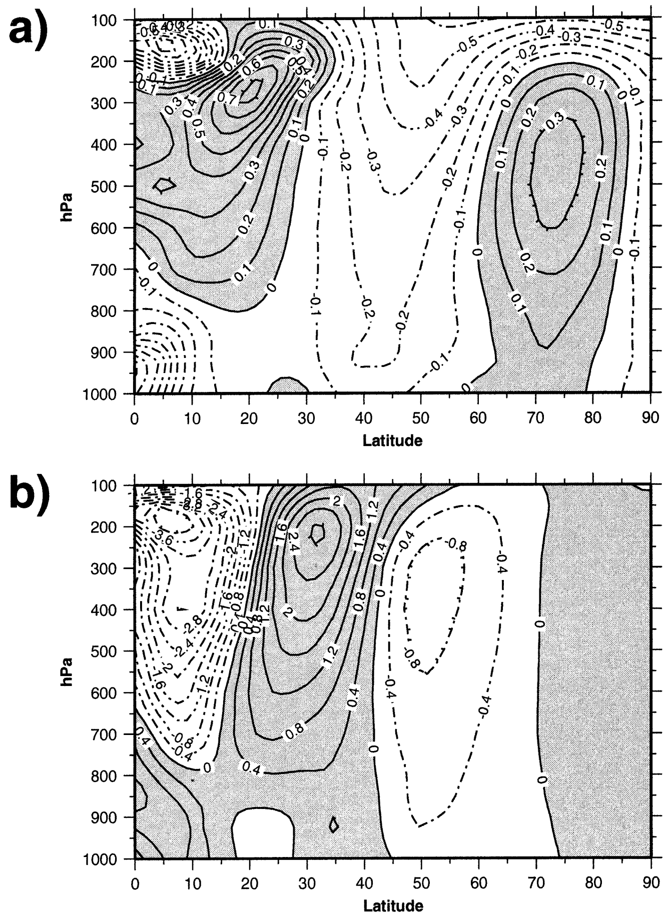

FIG. 12. Latitude–height cross section of the winter (DJF) difference field between the TAP and TAN for (a) meridional wind (m s^{-1}) and (b) zonal wind (m s^{-1}). The data are zonally averaged between 90° and 60°W. Shading indicates southerly and westerly winds in (a) and (b), respectively.

in the upward portion of the Ferrel cell south of 60°N (Fig. 12a). The anomalous convergence in the subtropics is associated with increased subsidence and anomalous drying of the lower troposphere (not shown). The TAD zonal wind shows a dipolar feature with anomalous easterlies in the tropical upper troposphere and anomalous westerlies in the subtropics with an equivalent barotropic structure (Fig. 12b).

b. The influence of stationary and transient planetary-scale waves

The advection of vorticity arising from the tropical wind divergence produces a significant Rossby wave source collocated with the subsiding branch of the anomalous Hadley outflow (Sardeshmukh and Hoskins 1988; Rasmusson and Mo 1993; Cassou 2001). This leads to an enhancement of stationary wave activity associated with warm TNA SST. To support this statement, dynamical diagnostics are computed, as in Pavan et al. (2000), and, in particular, the barotropic version of the generalized Eliassen–Palm (E–P; or stationary wave activity) flux as defined by Plumb (1985). As the response to the tropical Atlantic SST anomalies is mostly barotropic, an approximation of the generalized (E–P) flux to a barotropic atmosphere is applied to the 500-hPa flow. This index has been computed for individual monthly means and simulations and then, averaged to yield seasonal mean values. The TAD wave activity flux is shown in Fig. 13a superimposed onto the eddy component of the TAD geopotential anomaly. Warm TNA SST anomalies are associated with increased wave activity in the western Atlantic around 40°N as indicated by the strong divergence of the wave activity flux. Figure 13a also suggests enhanced wave activity propagating almost zonally into western Europe. It is worth noting that the more intense Hadley circulation is also related to changes in the transient eddy activity. The stronger subtropical jet and related enhanced vertical shear of the zonal wind in the subtropics lead to enhanced baroclinicity in the presence of a warm TNA SST anomaly. This, in turn, leads to enhanced eddy-

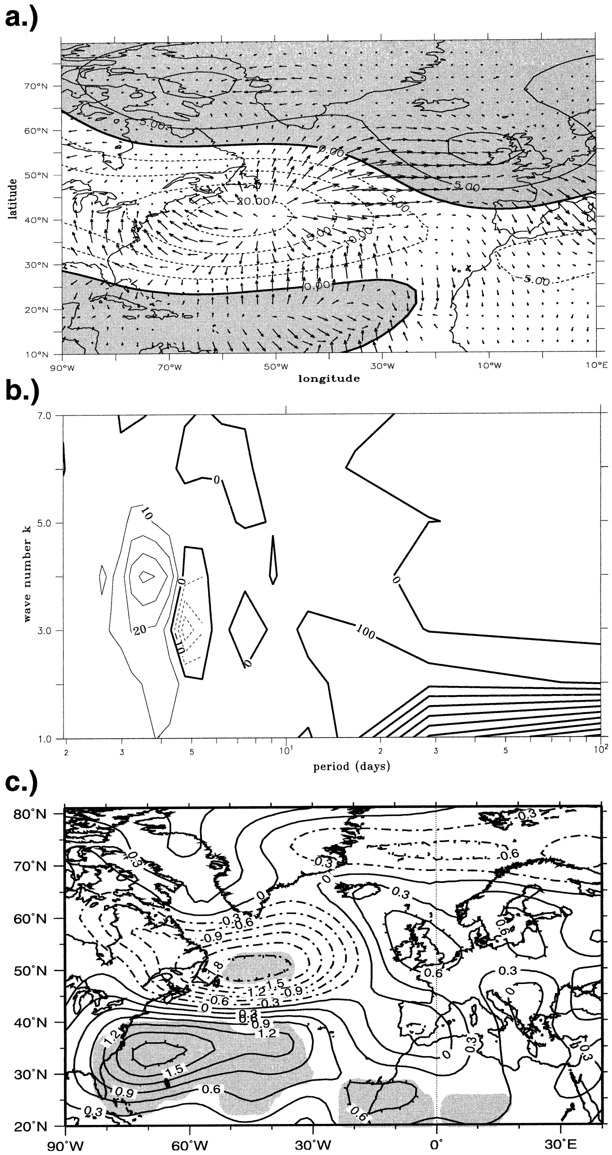

FIG. 13. Winter (DJF) difference field between the TAP and TAN for (a) wave activity flux computed from 500-hPa wind and geopotential height (arrows) superimposed onto the corresponding eddy anomalies of 500-hPa height (contours every 5 m), (b) frequency and zonal wave spectra of geopotential height transient fluctuations at 500 hPa and averaged between 25° and 40°N over a zonal domain ranging from 90°W to 90°E, and (c) storm track activity defined as the rms of bandpass (2.5–6 day) filtered 500-hPa height. Shading indicates positive eddy anomalies in (a) while in (c) it shows statistical significance using a two-tailed *t* test at the 95% confidence level. For the sake of clarity, the contour interval in (b) is 10 m^2 for the left side and 100 m^2 for the right side of the spectrum.

induced heat transport outside the Tropics leading to a reduced meridional temperature gradient at the midlatitudes. Figure 13b shows the relative importance of the synoptic-scale eddies versus the planetary-scale waves. The TAD variance spectra of the subtropical 500-hPa geopotential height shows an enhanced low-frequency response at wavenumbers 1–3 that peaks at periods greater than 30 days. This analysis thus suggests that the transient eddy response to warm TNA SST anomaly is dominated by low-frequency planetary-scale transients with a small contribution from the synoptic-scale eddies. The storm track activity is slightly enhanced off the east coast of the United States and reduced east of Newfoundland (Fig. 13c).

The indications from the previous diagnostics are that both the stationary and transient planetary-scale waves play an important role in the extratropical response to TNA SST anomalies. A key issue to be resolved concerns the physical processes responsible for the modulation of the stationary wave field. Changes in eddy activity located in the jet stream region suggest that the interaction with the transient eddies may be an important forcing mechanism through heat and momentum transports.

While the model MSLP response to tropical Atlantic SST anomalies is roughly linear over the western part of the basin, there is significant nonlinearity over the eastern Atlantic and Europe. The tropical atmosphere seems to react more strongly to warm SST anomalies as the 200-hPa streamfunction anomalies have an amplitude that is 50% greater in TAP relatively to TAN. In the TAP simulation, the dynamical diagnostics show an increased Rossby wave activity associated to a stronger northeastward propagation at high latitudes (not shown).

c. Synthesis

In summary, the results of this study can be synthesized into a picture of coupling between the tropical North Atlantic Ocean and the extratropical atmosphere over the NAE region during the northern winter. The physical mechanism involves, as was noted in an early observational analysis by Bjerknes (1966), a strong relation between the Hadley circulation intensity and the extratropical climate. Persistant tropical North Atlantic positive SST anomalies induce a strong enhancement of the convection activity over South America, north of the equator. The increased diabatic heating leads to an enhanced regional Hadley cell and to a stronger subtropical jet. This leads to an enhanced vertical zonal wind shear and increased baroclinicity in the western Atlantic region from the subtropics into the midlatitudes. These anomalies modulate the planetary-wave source and transient eddy activities as well as the related heat transport, leading to a reduced meridional temperature gradient at mid- to high latitudes (Hou 1998). Dynamical indices of planetary-wave forcing (such as the generalized Eliassen–Palm fluxes) show a clear propagation of the stationary wave activity from the subtropics into the mid- and high latitudes along a great circle path originating from the Caribbean into the northeast Atlantic. These diagnostics suggest that tropical processes associated with North Atlantic SST anomalies can play an active role in modulating the extratropical atmospheric circulation via changes in the tropical meridional circulation. The major role played by the modulation of the tropical convection may explain both the asymmetrical relationship coming from the cluster analysis and the nonlinearities in the TA(P/N) experiments, via the dependence of the atmospheric water vapor content versus temperature.

5. Conclusions

By analyzing the data coming from two ensembles of multidecadal integrations performed with the ARPEGE model, a systematic assessment of the effect of Atlantic SSTs on low-frequency atmospheric variability over the North Atlantic–European region is performed. In the first ensemble (GOGA), the observed SSTs and SIEs from the GISST dataset are prescribed globally while they are restricted to the Atlantic Ocean in the second ensemble (AOGA). A signal-to-noise maximizing EOF analysis is used to isolate the dominant forced response from the internal atmospheric variability. The method is applied to North Atlantic low-pass-filtered seasonal mean MSLP anomalies and the analysis is made for both the winter (DJF) and spring (MAM) seasons over the 1948–98 period. The principal findings of this study are the following.

1) The leading response in the GOGA simulations can be attributed to oceanic changes related to ENSO. The spatial pattern of the leading forced mode in winter exhibits a primary center of action located slightly north of the Azores archipelago and a secondary maximum off the Florida coast. The time series of the forced response is strongly correlated to the Niño-3 index.
2) In order to find out whether the local Atlantic SSTs do exert any influence on atmospheric variability over the NAE sector, two different approaches were used and compared. The ENSO influence was removed from the GOGA simulations with a simple linear regression of the MSLP data with the Niño-3 index and the EOF algorithm was applied to the residual part of the data. The EOF algorithm was also applied to the AOGA ensemble. A common detectable response is found in winter and to a lesser extent in spring. In fact, while the forced spring response from the AOGA ensemble is close to the common (GOGA and AOGA) winter signal, the forced spring GOGA response does not exhibit a large-scale coherent pattern. The characteristic temporal evolution of the winter response is also obtained from the application of the same algorithm to other atmospheric variables such as the AOGA Z500 and U200 fields. This temporal evolution shows quasi-decadal variability (with a period between 6 and 8 yr) superimposed on a lower-frequency fluctuation. It is also well correlated with fluctuations in a tripole pattern of SST anomalies in the North Atlantic.
3) The spatial structure of the leading forced response in winter is dominated by a large-scale dipole in MSLP, resembling the NAO structure but with a stronger midlatitude center of action. Applying the signal-to-noise maximizing EOF algorithm to other variables (Z500 and U200) shows a very coherent signal with a quasi-barotropic signature close to that of the NAO. The low-frequency changes between the first part of the period (1950–70) and the second part can be explained in terms of changes in the frequency of occurrence of a natural regime of atmospheric intraseasonal–interannual variability with a spatial structure very similar to that of the positive phase of the NAO.
4) The leading forced atmospheric response is induced primarily by the tropical part of the SST tripole as shown by the strong correlation between the tropical North Atlantic SST index and the characteristic temporal evolution of the forced response. To further confirm this finding, two 30-yr additional integrations were carried out with idealized SST anomalies representing the positive (TAP) and negative (TAN) phases of the tropical part of the SST tripole. Similarity between the difference (TAP − TAN) fields and the leading forced responses from the AOGA integrations demonstrate that the tropical North Atlantic SST anomalies can lead to changes that tend to reenforce the geopotential structure of the simulated NAO.
5) The physical mechanism involves related changes in tropical convection, Hadley circulation, and the modulation of the stationary planetary-scale waves by the low-frequency variability in subtropical winds induced by the persistent tropical circulation anomalies. Enhanced baroclinicity and related changes in planetary-scale transient eddies in the western subtropical North Atlantic may have a catalytic role in forcing and sustaining the anomalous stationary wave activity.

Although the present study suggests the influence of tropical North Atlantic SSTs onto the extratropical atmosphere, the extent to which the atmospheric response could feed back onto the tropical Atlantic remains to be explored. The strategy adopted here does not allow a complete representation of feedback processes because it only accounts for the atmospheric response to SST and SIE forcings and do not include oceanic processes. Diagnosing surface heat fluxes in SST forced atmospheric GCM integrations to evaluate these feedbacks can be erroneous due to the infinite heat source at the lower boundary (Barsugli and Battisti 1998). Further simulations with an AGCM coupled to various ocean components (mixed layer model or ocean GCM) are needed to quantify the potential feedbacks acting to produce low-frequency variability over the North Atlantic region.

Acknowledgments. We would like to thank Rowan Sutton, Andy Robertson, and Paco Doblas-Reyes for fruitful discussions and help regarding the statistical tools used in this study. We would also like to thank Sophie Valcke and Marie Drevillon for insightful discussions and help regarding the model data. This work was supported by the European Community via the 5th framework program PREDICATE Project under Contract EVK2-CT-1999-00020. Computer time was provided by the IDRIS and Météo-France computing centers.

REFERENCES

Alexander, M. A., and C. Deser, 1995: A mechanism for the recurrence of winter time midlatitude SST anomalies. *J. Phys. Oceanogr.,* **25,** 122–137.

Allen, M. R., and L. A. Smith, 1997: Optimal filtering in singular spectrum analysis. *Phys. Lett.,* **234,** 419–428.

Appenzeller, C., J. Schwander, S. Sommer, and T. F. Stocker, 1998: The North Atlantic Oscillation and its imprint on precipitation and ice accumulation in Greenland. *Geophys. Res. Lett.,* **25,** 1939–1942.

Barnston, A. G., and R. E. Livezey, 1987: Classification, seasonality and persistance of low-frequency atmospheric circulation patterns. *Mon. Wea. Rev.,* **115,** 1083–1126.

Barsugli, J. J., and D. S. Battisti, 1998: The basic effects of atmosphere–ocean thermal coupling on midlatitude variability. *J. Atmos. Sci.,* **55,** 477–493.

Bjerknes, J., 1964: Atlantic air–sea interaction. Vol. 10, *Advances in Geophysics,* Academic Press, 1–82.

——, 1966: A possible response of the atmospheric Hadley circulation to equatorial anomalies of ocean temperature. *Tellus,* **18,** 820–829.

Cassou, C., 2001: Rôle de l'océan dans la variabilité basse fréquence de l'atmosphère sur la région Nord Atlantique-Europe. Ph.D. dissertation, University of Paul Sabatier, Toulouse, France, 280 pp.

——, and L. Terray, 2001a: Dual influence of Atlantic and Pacific SST anomalies on the North Atlantic/Europe winter climate. *Geophys. Res. Lett.,* **28,** 3195–3198.

——, and ——, 2001b: Oceanic forcing of the wintertime low-frequency atmospheric variability in the North Atlantic European sector: A study with the ARPEGE model. *J. Climate,* **14,** 4266–4291.

Cayan, D. R., 1992a: Latent and sensible heat flux anomalies over the northern oceans: Driving the sea surface temperature. *J. Phys. Oceanogr.,* **22,** 859–881.

——, 1992b: Latent and sensible heat flux anomalies over the northern oceans: The connection to monthly atmospheric circulation. *J. Climate,* **5,** 354–369.

Chang, P., J. Li, and H. Li, 1997: A decadal climate variation in the tropical Atlantic ocean from thermodynamic air–sea interaction. *Nature,* **385,** 516–518.

——, R. Saravanan, L. Ji, and G. Hegerl, 2000: The effect of local SST on atmospheric circulation over the tropical Atlantic sector. *J. Climate,* **13,** 2195–2216.

Cook, E. R., R. D. D'Arrigo, and K. R. Briffa, 1998: A reconstruction of the North Atlantic Oscillation using tree-ring chronologies from North America and Europe. *Holocene,* **8,** 9–17.

Corti, S., F. Molteni, and T. N. Palmer, 1999: Signatures of recent climate change in frequencies of natural atmospheric circulation regimes. *Nature,* **398,** 799–802.

Déqué, M., C. Dreveton, A. Braun, and D. Cariolle, 1994: The climate version of Arpege/IFS: A contribution to the French community climate modelling. *Climate Dyn.,* **10,** 249–266.

Deser, C., and M. L. Blackmon, 1993: Surface climate variations over the North Atlantic ocean during winter. *J. Climate,* **6,** 1743–1753.

Enfield, D. B., and D. A. Mayer, 1997: Tropical Atlantic SST variability and its relation to El Niño–Southern Oscillation. *J. Geophys. Res.,* **102,** 929–945.

——, A. M. Mestas-Nuñez, D. A. Mayer, and L. Cid-Serrano, 1999: How ubiquitous is the dipole relationship in tropical Atlantic sea surface temperatures. *J. Geophys. Res.,* **104,** 7841–7848.

Ferranti, L., F. Molteni, and T. N. Palmer, 1994: Impact of localized tropical and extratropical SST anomalies in ensembles of seasonal GCM integrations. *Quart. J. Roy. Meteor. Soc.,* **120,** 1613–1645.

Frankignoul, C., 1985: Sea surface temperature anomalies, planetary waves and air–sea feedback in the middle latitudes. *Rev. Geophys.,* **23,** 357–390.

——, A. Czaja, and B. L'Hévéder, 1998: Air–sea feedback in the North Atlantic and surface boundary conditions for ocean models. *J. Climate,* **11,** 2310–2324.

Hansen, D. V., and H. F. Bezdek, 1996: On the nature of decadal anomalies in North Atlantic sea surface temperature. *J. Geophys. Res.,* **101,** 8749–8758.

Hoskins, B., and D. Karoly, 1981: The steady linear response of a spherical atmosphere to thermal and orographic forcing. *J. Atmos. Sci.,* **38,** 1179–1196.

Hou, A. Y., 1998: Hadley circulation as a modulator of the extratropical climate. *J. Atmos. Sci.,* **55,** 2437–2457.

Hurrell, J. W., 1995: Decadal trends in the North Atlantic Oscillation and relationships to regional temperature and precipitation. *Science,* **269,** 676–679.

——, and H. van Loon, 1997: Decadal variations in climate associated with the North Atlantic Oscillation. *Climate Change,* **36,** 301–326.

Jones, P. D., T. Jónsson, and D. Wheeler, 1997: Extension to the North Atlantic Oscillation using early instrumental pressure observations from Gibraltar and south-west Iceland. *Int. J. Climatol.,* **17,** 1433–1450.

Klein, S. A., B. J. Soden, and N. G. Lau, 1999: Remote sea surface temperature variations during ENSO: Evidence for a tropical atmospheric bridge. *J. Climate,* **12,** 917–932.

Kushnir, Y., 1994: Interdecadal variations in North Atlantic sea surface temperature and associated atmospheric conditions. *J. Climate,* **7,** 141–157.

——, and N. C. Lau, 1992: The general circulation model response to a North Pacific SST anomaly: Dependence on timescale and pattern polarity. *J. Climate,* **5,** 271–283.

——, and I. M. Held, 1996: Equilibrium atmospheric response to North Atlantic SST anomalies. *J. Climate,* **9,** 1208–1220.

——, W. A. Robinson, I. Bladé, N. M. J. Hall, S. Peng, and R. T. Sutton, 2002: Atmospheric GCM response to extratropical SST anomalies: Synthesis and evaluation. *J. Climate,* **15,** 2233–2256.

Lau, N. C., and M. J. Nath, 1994: A modeling study of the relative role of tropical and extratropical SST anomalies in the variability of the global atmosphere–ocean system. *J. Climate,* **7,** 1184–1207.

Marshall, J. C., and F. Molteni, 1993: Toward a dynamical understanding of weather regimes. *J. Atmos. Sci.,* **50,** 1792–1818.

Martineu, C., J. Y. Caneill, and R. Sadourny, 1999: Potential predictability of European winters from the analysis of seasonal simulations with an AGCM. *J. Climate,* **12,** 3033–3061.

Mehta, V. M., M. J. Suarez, J. V. Manganello, and T. Delworth, 2000: Oceanic influence on the North Atlantic Oscillation and associated Northern Hemisphere climate variations: 1959–1993. *Geophys. Res. Lett.,* **27,** 121–124.

Michelangeli, P., R. Vautard, and B. Legras, 1995: Weather regime recurrence and quasi stationarity. *J. Atmos. Sci.,* **52,** 1237–1256.

Nobre, P., and J. Shukla, 1996: Variations of sea surface temperature, wind stress, and rainfall over the tropical Atlantic and South America. *J. Climate,* **9,** 2464–2479.

Okumura, Y., S. P. Xie, A. Numaguti, and Y. Tanimoto, 2001: Tropical

Atlantic air–sea interaction and its influence on the NAO. *Geophys. Res. Lett.,* **28,** 1507–1510.
Palmer, T. N., and Z. Sun, 1985: A modelling and observational study of the relationship between sea surface temperature in the North West Atlantic and the atmospheric general circulation. *Quart. J. Roy. Meteor. Soc.,* **111,** 947–975.
Pavan, V., F. Molteni, and C. Brankovic, 2000: Wintertime variability in the Euro-Atlantic region in observations and in ECMWF seasonal ensemble experiments. *Quart. J. Roy. Meteor. Soc.,* **126,** 2143–2173.
Peng, S., and J. S. Whitaker, 1999: Mechanisms determining the atmospheric response to midlatitude SST anomalies. *J. Climate,* **12,** 1393–1408.
——, L. A. Mysak, H. Ritchie, J. Derome, and B. Dugas, 1995: The differences between early and midwinter responses to sea surface temperature anomalies in the northwest Atlantic. *J. Climate,* **8,** 137–157.
——, W. A. Robinson, and M. P. Hoerling, 1997: The modeled atmospheric response to midlatitude SST anomalies and its dependence on background circulation states. *J. Climate,* **10,** 971–987.
Plumb, R., 1985: On the three-dimensional propagation of stationary waves. *J. Atmos. Sci.,* **42,** 217–228.
Rasmusson, E. M., and K. Mo, 1993: Linkages between the 200-mb tropical and extratropical circulation anomalies during the 1986–1989 ENSO cycle. *J. Climate,* **6,** 595–616.
Rayner, N. A., E. B. Horton, D. E. Parker, C. K. Folland, and R. B. Hackett, 1997: Version 2.2 of the Global Sea-Ice and Sea Surface Temperature data set, 1903–1994. Hadley Centre, Met Office CRTN 74, 21 pp.
Robertson, A. W., C. Mechoso, and Y. Kim, 2000: The influence of Atlantic sea surface temperature anomalies on the North Atlantic Oscillation. *J. Climate,* **13,** 122–138.
Rodwell, M. J., D. P. Rowell, and C. K. Folland, 1999: Oceanic forcing of the wintertime North Atlantic Oscillation and European climate. *Nature,* **398,** 320–323.
Rogers, J. C., 1984: The association between the North Atlantic Oscillation and the Southern Oscillation in the Northern Hemisphere. *Mon. Wea. Rev.,* **112,** 1999–2015.
——, 1990: Patterns of low-frequency monthly sea level pressure variability (1899–1986) and associated wave cyclone frequencies. *J. Climate,* **3,** 1364–1379.
Saravanan, R., and P. Chang, 2000: Interaction between tropical Atlantic variability and El Niño–Southern Oscillation. *J. Climate,* **13,** 2177–2194.
Sardeshmukh, P. D., and B. J. Hoskins, 1988: The generation of global rotational flow by steady idealized tropical divergence. *J. Atmos. Sci.,* **45,** 1228–1251.
Stephenson, D. B., V. Pavan, and R. Bojariu, 1999: Is the North Atlantic Oscillation a random walk? *Int. J. Climatol.,* **20,** 1–18.
Sutton, R. T., and M. R. Allen, 1997: Decadal variability of North Atlantic sea surface temperature and climate. *Nature,* **388,** 563–567.
——, W. A. Norton, and S. P. Jewson, 2001: The North Atlantic Oscillation—What role for the ocean? *Atmos. Sci. Lett.,* **1,** 89–100.
Terray, L., and C. Cassou, 2000: Modes of low frequency climate variability and their relationships with land precipitation and surface temperature: application to the Northern Hemisphere Winter climate. *Stoch. Environ. Res. Risk Assess.,* **14,** 339–369.
Venzke, S., M. R. Allen, R. T. Sutton, and D. P. Rowell, 1999: The atmospheric response over the North Atlantic to decadal changes in sea surface temperature. *J. Climate,* **12,** 2562–2584.
Wallace, J. M., and Q. Jiang, 1987: On the observed structure of the interannual variability of the atmosphere–ocean climate system. *Atmospheric and Oceanic Variability,* H. Cattle, Ed., Royal Meteorological Society, 17–43.
Watanabe, M., and M. Kimoto, 1999: Tropical–extratropical connection in the Atlantic atmosphere–ocean variability. *Geophys. Res. Lett.,* **26,** 2247–2250.
Wunsch, C. J., 1999: The interpretation of short climate records, with comments on the North Atlantic and Southern Oscillation. *Bull. Amer. Meteor. Soc.,* **80,** 245–255.